Chalcogenide Letters Vol. 13, No. 6, June 2016, p. 247 - 255

# STRUCTURAL CHARACTERISATION AND OPTICAL PROPERTIES OF ANNEALED ZnSSe THIN FILMS

A. A. AKL[a,b], S. A. ALY[a*], H. HOWARI[c,d]
[a]*Physics Department, Faculty of Science, Minia University, Minia, Egypt*
[b] *Faculty of Science in Ad-Dawadmi, Physics Department, Shaqra University, 11911, KSA*
[c] *Physics Department, Faculty of Science, Al-Baath University, Homs, Syria*
[d] *Physics Department, Faculty of Science, Qassim University, Buraidah, Kingdom of Saudi Arabia*

ZnSSe thin films were thermally evaporated on unheated quartz substrates using ZnS/ZnSe thin film layers. The prepared films were subjected to post deposition pulsed laser annealing (PLA) at different powers of 15, 20 and 30W. XRD analysis indicates that all ZnS/ZnSe layers after annealing possess a single phase cubic structure with a strong preferred (111) orientation. The evaluated average crystallite size as deduced from the FWHM of the XRD layer peaks was varied from 26.5 nm for the as deposited sample to 34.80 nm for the sample annealed at PLA power of 30 W. The optical characteristics of the samples were studied by measuring the spectral transmittance and reflectance. The optical energy gap as well as refractive index were measured and then correlated with the PLA power.

(Received March 26, 2016; Accepted June 4, 2016)

Keywords: ZnSSe thin films, Annealing, Thermal evaporation, Crystallization, Optical energy gap.

## 1. Introduction

II–VI semiconductors are extensively studied due to their numerous applications in light-emitting as well as laser diodes [1–3]. Due to wider band-gap, II-VI compound multilayer structures are candidate to be applied in numerous optoelectronic devices [4-6]. ZnS is wide-band-gap semiconductor that can be used for the detection, emission and modulation of visible and UV light [7,8]. When ZnS combines with other materials such as ZnSe, it produces a stimulating and potentially effective heterostructures such as ZnS/ZnSe systems. The presence of sulfur in ZnSSe widens the band gap, which increases the blue response of devices [9]. ZnSSe can be used as a wavelength tunable UV photo detector, light emitters, visible laser diodes and light emitting diodes [10].

Pulsed laser annealing (PLA) of semiconductors was first carried out to eliminate the damage caused by the ion implantation [11-12]. Nevertheless, laser crystallization techniques were far more successful in converting amorphous Si or polycrystalline Si into a single-crystal Si because the kinetic energies of laser power are able to improve the crystallinity of the as grown films [13,14]. Moreover, PLA process has the ability of producing materials with impurities concentration over the natural solubility limit. This is due to the rapid heating and cooling occurrence in the material which causes recrystallization, where substitution impurities diffuse into native lattice sites. In this work, the growth of ZnSSe thin films on quartz substrates by the physical evaporation technique was carried out using a ZnS/ZnSe heterostructures. The as deposited films were subjected to post deposition pulsed laser annealing (PLA) of different powers to get a single phase of ZnSSe. The film microstructure were described by X-ray diffraction and the optical properties was also studied and discussed.

*Corresponding author: saaly61@hotmail.com

## 2. Experimental work

ZnSSe samples of the same film thickness were thermally deposited on unheated ultrasonically cleaned quartz substrates using bilayers of ZnS and ZnSe of high purity (99.999%) using Edwards coating unit (type E306A). A tungsten boat was used as a heating filament . The evaporation process has been performed at a vacuum of about of $8.2 \times 10^{-4}$ Pa.

In order to study the effect of PLA on the structure and optical properties of the investigated films, the annealing process was carried out at different pulsed laser powers namely 15, 20 and 30W.

A quartz crystal oscillator are used to monitor both the film thickness and deposition rate. The ratios of individual layer thicknesses were 1.0:1.48 to achieve a 1:1:1 stoichiometric ratio for Zn, S and Se, respectively. The total film thickness of each sandwich was about 335nm (thickness of ZnS=135nm and ZnSe=200nm).

A JEOL X-ray diffractometer (Model JSDX-60PA) with a Ni filter Cu-$k_\alpha$ radiation ($\lambda$ = 0:15418 nm) was used. Continuous scanning was applied with a slow scan speed of $1^o$/min with a relatively small time constant (1sec). A scanning range of $2\Theta$ from 6 to $72^o$ was used. The crystallite size as well as microstrain of the films were estimated using Debye-Scherrer formula [15]. The diffraction plane (111) characterizing the XRD patterns of the annealed films were used for the calculation.

A Jasco double beam spectrophotometer (V-570) was used to perform the spectral transmittance, T($\lambda$), and reflectance, $R(\lambda)$, in the spectral range from 280 to 800 nm. All optical measurements have been performed at room temperature (300 K).

The following relation [16] is used to calculate the absorption coefficient ($\alpha$)

$$\alpha = \frac{1}{t}\ln\left(\frac{(1-R(\lambda)}{T(\lambda)}\right) \tag{1}$$

where $t$ is the film thickness.

## 3. Results and discussion:

### 3.1. Formation of ZnSSe single phase:

The XRD diffraction patterns for some ZnS/ZnSe samples in the as deposited state and after annealing at different laser powers are shown in Fig. 1. For the as-deposited sample, a major peaks are seen at about 27.25° and $28.64^o$ which corresponds to (111) plane reflections from cubic type zinc blende for both ZnSe and ZnS phases. Also, two other peaks are observed for free phases of both of ZnSe and ZnS at about $45.35^o$, $47.62^o$ , $53.72^o$ and $56.35^o$ corresponds to (220) and (311) plane respectively. Comparing the observed 'd' values with standard 'd' values (PDF number 05-0566 and 05-0522) indicates that the ZnS and ZnSe samples are polycrystalline and possess a cubic (zinc blende) structure. This fact indicates that the two layers of ZnS and ZnSe are stacked without solid reactions. After pulsed laser annealing, a major peak is observed at $2\Theta = 27.80^o$ (111) at different PLA powers. Furthermore, the structure is improved and the degree of orientation of crystallites increases (an increase of peak intensities corresponding to (111) planes of ZnSSe take place). It can be, also, revealed from the spectrum that the layers possess only ZnSSe phase. Also, no considerable change in the position of the (111) peak was noticed with increasing PLA power.

The evaluated inter-planar spacing and lattice constant were 3.209Å and 5.558Å, respectively. These values showed a relatively small variation if compared with single crystal ZnSSe [17], which may be attributed to the misfit of thermal strain between the film and the substrate. This result is analogous to that reported on $ZnS_xSe_{1-x}$ films [18-23].

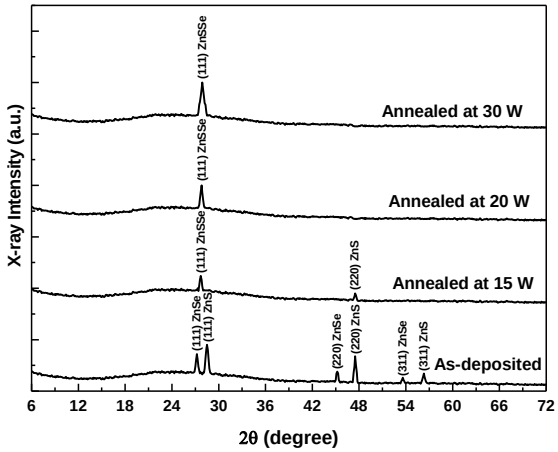


*Fig. 1: X-ray diffraction pattern for the as-deposited sample as well as for samples annealed at PLA powers of 15, 20 and 30W*

The average crystallite size, D, of the ZnSSe films formed at 15, 20 and 30W along the direction of the (111) plane was estimated using the full width at half maxima (FWHM) values using Debye-Scherrer formula [15];

$$D = \frac{0.94\lambda}{\beta \cos\theta} \tag{2}$$

where β is the value of FWHM of (111) peak of XRD pattern, λ is the wavelength of x-ray (λ = 0.154184nm)

The dislocation density (δ) can be defined as the length of dislocation lines per unit volume, and is calculated using the following equation [24, 25]

$$\delta = \frac{1}{D^2} \tag{3}$$

The values of the dislocation density of matter are a measure of amount of defects in the crystal. The number of crystallites per unit area (N) and the microstrain (ε) of the investigated samples were estimated using the following formulas [26]:

$$N = \frac{t}{D^3} \tag{4}$$

$$\varepsilon = \frac{\beta \cos\theta}{4} \tag{5}$$

where t is the film thickness.

The effect of PLA power on the average crystallite size and internal microstrain are shown in Figs. 2 and 3 respectively. It can be noticed that the average crystallite size is varied from 26.5 nm in the as-deposited state to 34.8 nm for films annealed at PLA of 30W. The increase in the average crystallite size with the laser power indicates an improvement in crystallinity. In contrast, the amount of internal microstrain is found to decrease with increasing PLA power as shown in Fig. 3. The value of microstrain is decreased from $1.37 \times 10^{-3}$ for the as-deposited sample to $1.04 \times 10^{-3}$ for the sample annealed at PLA of 30W. This is because the microstrain is equivalent to variations in the d-spacing within domains by an amount depending on the elastic constants of

the material and the nature of internal stresses, which is decreased with increasing annealing powers.

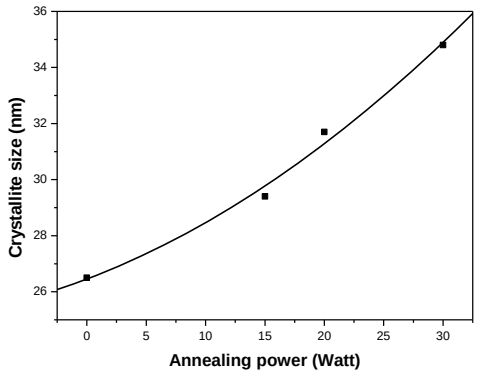


*Fig. 2: The average crystallite size with annealing power*

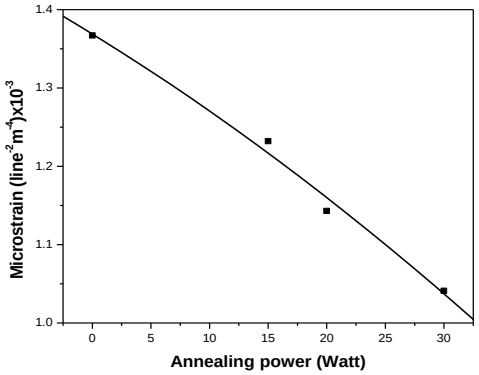


*Fig. 3: The microstrain with annealing power*

The calculated values of structural parameters of the as-deposited and annealed samples are depicted in Table (1). It can be noticed from the table that the dislocation density, δ, is decreased from $14.24x10^{14}$ for the as-deposited sample to $8.26x10^{14}$ (lines/$m^2$) after annealing at PLA of 30 W. Also, it can be noticed from Table (1) that the number of crystallites per unit area (N) is decreased with increasing PLA power and its value is ranged between $18x10^{15}$ and $7.95x10^{15}$ crystallite/$m^2$.

*Table (1): Structural parameters of ZnSSe thin films as a function of annealing power*

| annealing Power | Average crystallite Size (nm) | Broadening (radian) | Microstrain [line$^{-2}$m$^{-4}$] x$10^{-3}$ | Dislocation density x$10^{14}$ (line/$m^2$) | Number of crystallite (x$10^{15}$)/$m^2$ |
|---|---|---|---|---|---|
| As-deposited | 26.5 | $5.634x10^{-3}$ | 1.367 | 14.240 | 18.00 |
| 15 W | 29.4 | $5.078 x10^{-3}$ | 1.232 | 11.570 | 13.18 |
| 20W | 31.7 | $4.710 x10^{-3}$ | 1.143 | 9.951 | 10.52 |
| 30W | 34.8 | $4.290 x10^{-3}$ | 1.041 | 8.257 | 7.95 |

### 3.2. Optical properties:

#### *3.2.1. Trnsmittance and reflectance measurements:*

The variation in spectral transmittance and reflectance for the as deposited sample as well as for the annealed samples are shown in Fig. 4. It was observed that multiple interference fringes

are obtained in the transmittance of the investigated films. This is a result of multiple reflections at the substrate/film interface, i.e. due to different refractive index of ZnSSe and substrate. Moreover, the increase of annealing powers decreases the transmittance, which means that the crystallization improves the absorption. Furthermore, a small variation in the reflectance value with wavelength is noticed for all samples.

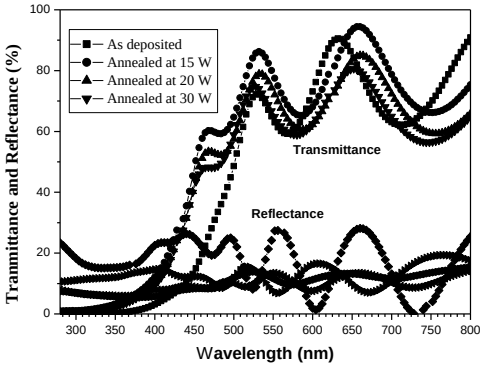


*Fig. 4: Dependence of spectral transmittance and reflectance on wavelength*

### *3.2.2. The absorption coefficient:*

Equation (1) is used to calculate the absorption coefficient and its variation with wavelength for samples annealed at different PLA powers is obtained in Fig.5. There is no appreciable change in the values of the absorption coefficient is observed for wavelengths $\geq$ 450 nm . For $\lambda$ < 450 nm, the value of $\alpha$ is remarkably dependent on wavelength. The dramatic increase in, $\alpha$, in this range can be attributed to the transition across ZnSSe band gap.

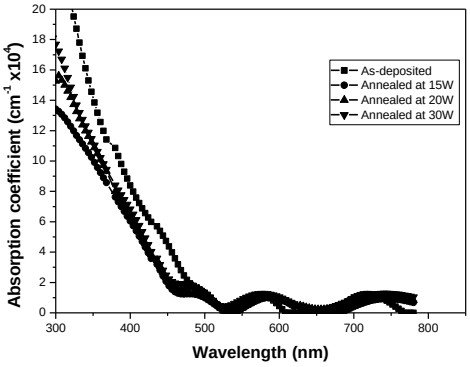


*Fig. 5: Variation of absorption coefficient with wavelength*

### *3.2.3. Optical energy gap*:

The optical energy gap ($E_g$) of the investigated samples is calculated from the following classical relation

$$\alpha = \frac{A(h\nu - E_g)^{1/2}}{h\nu} \tag{6}$$

where A is a constant.

The dependence of $(\alpha h\nu)^2$ on the photon energy ($h\nu$) is depicted in Fig. 6 for the as-deposited sample and for the samples annealed at PLA power of 15, 20 and 30 W, respectively. The value of the energy gap is obtained from the extrapolation of the linear portion with the photon energy axis. This plot indicates a direct allowed transition. The

correlation of the energy gap value with PLA power is shown in Fig. 7. An increase in $E_g$ value from 3.05 for the as-deposited sample to 3.3 eV for the sample annealed at PLA power of 30W. These values for $E_g$ are similar to those reported elsewhere [20-22].

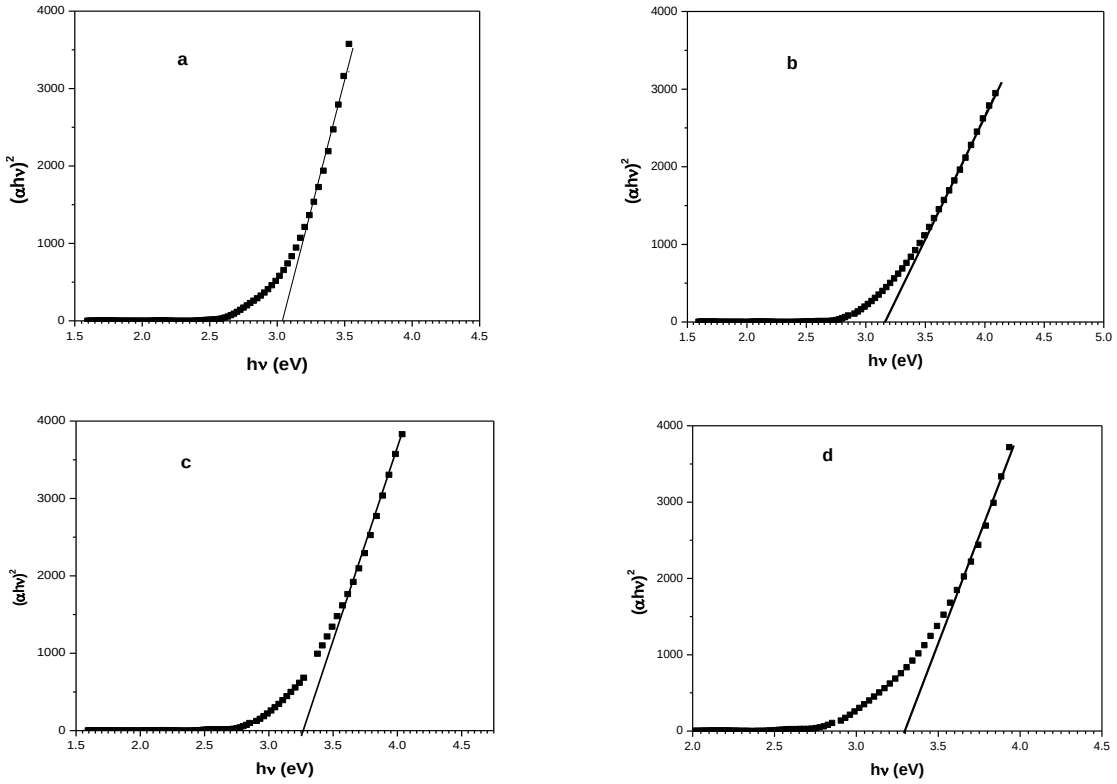


*Fig. 6: $(\alpha h\nu)^2$ with photon energy $(h\nu)$ for a) As-deposited sample b)sample annealed at PLA power of 15W c) sample annealed at PLA power of 20W d) sample annealed at PLA power of 30W.*

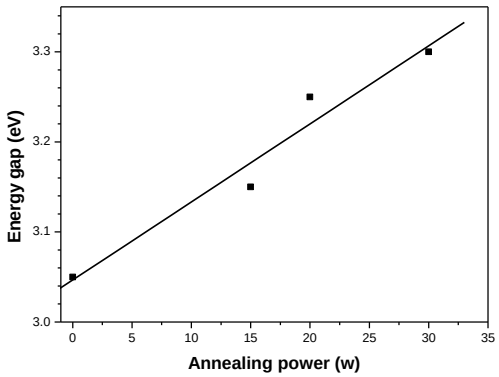


*Fig.7: Variation of optical energy gap with PLA power.*

The increase in the value of band gap energy could be attributed to the existence of high-density levels within the band gap [27] and the quantum confinement effects caused by the structural changes in the films with annealing [ 28-30].

### *3.2.4. Refractive index*

The refractive index, n of the investigated samples is estimated from the corrected T(λ) and R(λ) using Murmann's exact equation [31].

The dependence of the fitted values of refractive index on wavelength at different laser powers is shown in Fig. 8. It is noticed that the value of refractive index is quite high at low wavelengths (strong absorption) for all samples. This behavior may be attributed to the equality between the frequency of incident electromagnetic radiation and the a frequency [32]. At longer wavelengths, λ > 600nm, no appreciable change was observed. This behavior is in good agreement with the data obtained elsewhere [33-35] for like phase.

The dependence of n ( at λ = 550 nm) on annealing power is depicted in Fig.9. it can be noticed that the value of refractive index increases with increasing annealing power. This increase could be attributed to the increase of crystallite size and the reduction of dislocation density with annealing [36].

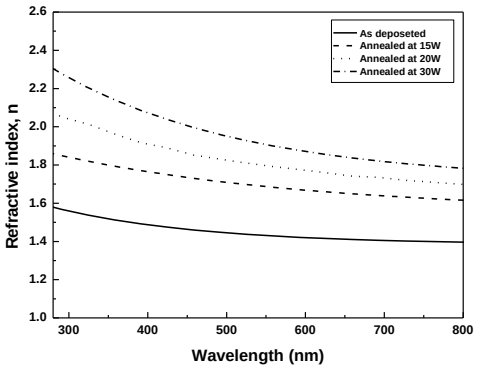


*Fig. (8): Refractive index (n) with wavelength at different PLA powers.*

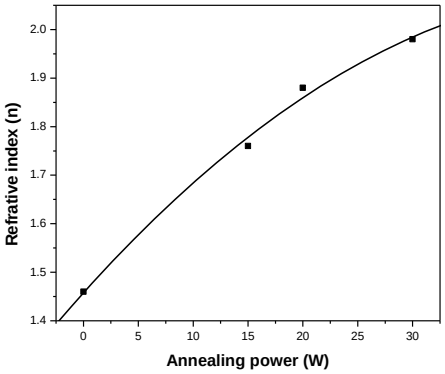


*Fig. (9): Refractive index (n) at 550 nm as a function of annealing power.*

## 4. Conclusion

Polycrystalline ZnSSe *films* of the same film thickness (335 nm) were grown by thermal evaporation technique on quartz substrates at room temperature. The films were subjected to post-deposition pulsed laser annealing (PLA) at different powers in the range 15–30W. The XRD analysis demonstrated that, all the ZnS/Se layers after annealing were polycrystalline, single phase with cubic structure. These films possess a strong preferred (111) orientation. The average crystallite size was varied in the range

26.54 – 34.80 nm for the as grown sample and that annealed at PLA power of 30W respectively.

A slight increase in the energy gap value is achieved from 3.05 eV for the as-deposited sample to 3.3 eV for the sample annealed at PLA power of 30 W. The refractive index (n) was found to be affected by annealing power. An increase in the value of n as PLA power increases. This increase was attributed to the increase of crystallite size as well as the decrease in dislocation density with increasing annealing power.

## References


[1] Z. Liu, M. Osamura, T. Ootsuka, R. Kuroda, Y. Fukuzawa, N. Otogawa, Y. Nakayama, Y. Makita, H. Tanoue, J. Cryst. Growth **307**, 82 (2007). .

[2] X.L. Zhu, L.W. Guo, N.S. Yu, J.F. Yan, M.Z. Peng, J. Zhang, H.Q. Jia, H. Chen, J.M. Zhou, J.Cryst. Growth **306**, 292 (2007.

[3] S. Armstrong, P.K. Datta, R.W. Miles,in: Proceedings of the 17th European Photovoltaic Solar Energy Conference, 22–26 October, **1184** (2001).

[4] Y.K. Liu, J.A. Zapien, Y.Y. Shan, C.Y. Geng, C.S. Lee, S.T. Lee, Adv. Mater. **17**, 1372 (2005).

[5] P.X. Gao, Y. Ding, Z.L. Wang, Nano Lett. **3**, 1315 (2003).

[6] A.L. Pan, H. Yang, R.B. Liu, R.C. Yu, B.S. Zou, Z.L. Wang, J. Am. Chem. Soc. **12**7, 15692 (2005)

[7] Y.F. Nicolau, M. Dupuy, M. Brunel, *J. Electrochem. Soc.*, **137**, 2915 (1990).

[8] E. Marquerdt, B. Optiz, M. Scholl, M. Henker, *J. Appl. Phys.* **75**, 8022 (1994).

[9] Y.P. Venkata Subbaiah, K.T. Ramakrishna Reddy, Mater. Chem. Phys. **92**, 448 (2005).

[10] O. Senthi Kumar, S. Soundeswaran, R. Dhanasekaran, Mater. Chem. Phys. **87**, 75(2004).

[11] P. Bhattacharya, L.Y. Pang, Phys. Today **47**, 64 (1994).

[12] R. A. Smith, Semiconductors, Cambridge University Press, Ch. **10**, 290 (1979).

[13] K. T. Ramakrishna Reddy, Y. V. Subbaiah, Thin Solid Films, 431-432, 340 (2003).

[14] H. Howari, D. Sands, J. E. Nicholls, J. H. C. Hogg, T. Stirner, and W. E. Hagston., J Appl. Phys. **88**, 1373 (2000).

[15] H.P.Klug, L.E. Alexander, X-ray Diffraction Procedures, Wiley, New York, (1954).

[16] F. Demichelis, G. Kaniadakis, A. Tagliferro, E. Tresso, Journal of Applied Optics, **26**, 737 (1987).

[17] V. Kumar, T.P. Sharma, Opt. Mater. **10**, 253 (1998).

[18] M. Ambrico, D. Smaldone, C. Spezzacatenna, V. Stagno, G. Perna, V. Capozzi, Semicon. Sci. Technol. **13**, 1446 (1998).

[19] S. Armstrong, P.K. Dutta, R.W. Miles, Thin Solid Films 403–404, 126 (2002).

[20] Y.P. Venkata Subbaiah, K.T. Ramakrishna Reddy, Materials Chemistry and Physics **92** (2005) 448.

[21] J. Ihanus, M. Ritala, M. Leskela, E. Rauhala, Appl. Surf. Sci. **112**, 154 (1997).

[22]S. Fridjine,S.Touihri,K.Boubaker, M.Amlouk, Journal of Crystal Growth **312**, 202 (2010).

[23] C.Wei Huang, H. Mei Weng, Y.Long Jiang, H. Yih Ueng, Thin Solid Films, **517**, 3667 (2009).

[24] A. Kropid owska, J. Chojnacki, A. Fahmi, B. Becker, Dalton Trans. **47**, 6825 (2008).

[25] V. Bilgin, S. Kose, F. Atay, I. Akyuz, Mater. Chem. Phys**. 94**, 103 (2005).

[26] Z.R. Khan, M. Zulfequar, Mohd. Shahid Khan, Mater. Sci. Eng. **B 174**, 145 (2010).

[27] L.Y. Sun, L.K. Kazamerski, A.H. Clark, P.J. Ireland, D.W. Morton, J. Vac. Sci Technol **15** (1978) 265.

[28] K. Prabhakar, Sa.K. Narayandass, D. Mangalaraj, J. Alloys Compd. **364**, 23 (2004).

[29] G.L. Tan, J. H. Du, Q.J. Zhang, J. Alloys Compd. **468**, 421(2009).

[30] S. Thangavel, S. Ganesan, S. Chandramohan, P. Sudhagar, Y.S. Kang, C.-H. Hong, J.

Alloys Compd. **495**, 234 (2010).
[31] O.S. Heavens, Optical Properties of Thin Films, Dover, New York, (1965).
[32] A. A. Akl, Journal of Physics and Chemistry of Solids, **71**, 223 (2010).
[33] K.M.M. Abo-Hassan, M.R. Muhamad , S. Radhakrishna, Thin Solid Films **491**, 117 (2005).
[34] C. Mehta, G.S.S. Saini, J. M. Abbas, S.K. Tripathi, Applied Surface Science **256**, 608 (2009).
[35] G.I. Rusu, M. Diciu, C. Pirghie, E.M. Popa, App. Surf. Science **253**, 9500 (2007).
[36] M. Ashraf, S.M.J. Akhtar, A.F. Khan, Z. Ali, A. Qayyum, J. Alloys and Compounds **509**, 2414 (2011).